한국지반공학회논문집 제16권 제4호 2000년 8월 PP. 201 ~208

Measurement of Pile Load Transfer Using Fiber Bragg Grating Sensor

광섬유 격자소자에 의한 말뚝의 하중전이 측정

Oh, Jeong-Ho 오 정 호*1 Lee, Won-Jae 이 원 제*2
Lee, Sang-Bae 이 상 배*3 Lee, Woo-Jin 이 우 진*4

요 지

본 연구에서는 광섬유 센서의 일종인 광섬유 격자소자(Fiber Bragg Grating sensor)를 모형말뚝에 설치하고 말뚝의 하중전이 측정을 시도하였다. 말뚝의 축방향 하중 및 주면 마찰력의 분포를 측정/분석시 사용되고 있는 스트레인 게이지에 의한 방법에 비해 광섬유 격자소자는 한 라인에 여러 개의 센서를 설치함으로써 여러 지점을 동시에 측정할 수 있다는 것과 센서의 설치가 용이하다는 장점을 가지고 있다. 본 연구에서 광섬유 격자소자와 스트레인 게이지를 모형말뚝에 함께 매설하고 재하시험중 하중전이를 측정한 결과, 두 측정치가 상당히 유사한 경향을 보였으며, 센서의 생존정도와 설치의 용이성에 있어서는 광섬유센서가 우수한 결과를 보였다. 따라서, 광섬유 격자소자의 말뚝 하중전이 측정에 대한 적용 가능성이 충분한 것으로 결론지었다.

Abstract

Axial load distribution in model piles was measured by Fiber Bragg Grating(FBG) sensor to investigate a possibility of analyzing the load transfer mechanism by Fiber Optic Sensor system. Since FBGs of different wave lengths can be multiplexed in an optical fiber, the installation of sensor system and the measurement of strains are relatively simple, compared with consisting strain gages. In this study, FBG sensors and electric strain gages were embedded in the same piles and the distributions of load transfer by two sensor systems were measured. It was observed from the test results that the variations of axial load by both systems showed insignificant difference and that the measurements by FBG were smoother than those by strain gage. Under the environments of laboratory testing, survival rate of embedded FBG system was higher than that of strain gage. Therefore, it was concluded that the use of FBG sensor has a great potential for the measurement of load transfer for pile foundation.

Keywords : Fiber optic sensor, Fiber bragg grating, Load transfer, Model pile

1. Introduction

Through the monitoring of geo-structures, geotechnical engineers usually obtain the information on the state of those structures and reevaluate the design parameters used. While strain gages usually measure the strains accurate enough for eneral purposes, simultaneous measurement of strains at several locations causes difficulties of embeddment of gages in a structure and of the line connection to measuring system at remote location. While the use of conventional

*1 정회원, 전 고려대학교 대학원 토목공학과
*2 정회원, 고려대학교 대학원 토목공학과 박사과정
*3 한국과학기술연구원 광기술연구센터 센터장
*4 정회원, 고려대학교 공과대학 토목환경공학과 부교수

strain gages is still popular, the applications of fiber optic sensor system to civil engineering structures have been aining ground. Several types of fiber optic sensor have been developed with the advance of fiber optic sensor technology and they have been mainly applied to the composite structures. Fiber optic sensor can measure an infinitesimal deformation with its high sensitivity to compressive and tensile deformations, and the multiplexing of several sensors in an optical fiber significantly reduces the complex arrangement of lead lines to remote data acquisition system.

In this research, static pile load tests were performed on model piles in which two sensor systems were embedded and the load transfer results by both systems were compared. A tension test of steel bar and a compression test of mortar specimen were also carried out to study the method of attachment of sensor in the structure and the relationship between the variation of FBG wavelength and strain.

2. Fiber Optic Sensors

2.1 Fiber Optic Components

Fiber optic cable transmitting the light is composed of core, cladding and buffer, as shown in Figure 1. Most of the cables are glass while plastic cables are used in some limited applications. The core carries the optical signal and the size of core varies, depending on cable types. Single mode cable, used for long range transmission of light and high bandwidth systems, has a core size of 8 to 10㎛. Multi-mode cable, used for shorter range, has a core size of 62.5㎛. The cladding keeps the light within the core, and prevents external light from entering the core. This layer, typically 125㎛ in diameter, is a glass similar to the core, but with a slightly different composition. Surrounding the cladding is a buffer layer that protects the inner glass. The buffer diameter is 900 ㎛, made of ceramic or plastic.

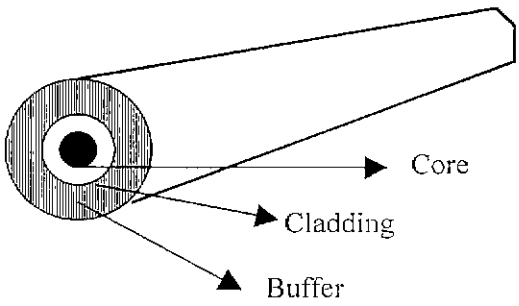

Fig. 1 Structure of Fiber Optic Cable

2.2 Fiber Bragg Grating Sensor(FBG)

FBG sensor is made by exposing the optical fiber of about 1cm long to the interference pattern of two coherent UV beams as shown in Figure 2. The absorption of UV light in the fiber changes the chemical bonds in the glass, thus causing the change in the refractive index of the glass. The resulting spatial modulation of refractive index produces the Bragg grating and acts as a narrow band in-line wavelength notch filter.

When the light signal from broad band source is transmitted, FBG reflects the signal of wavelength, λ_B, at which the Bragg resonance is satisfied, as shown in Figure 2. This Bragg resonance is determined by the condition:

$$\lambda_B = 2n\Lambda = \frac{n\lambda_L}{\sin(\theta/2)} \quad (1)$$

where Λ is spatial pitch of grating, n is refractive index of fiber, λ_L is the larger wavelength, and θ is the angle between beams. Refractive index is dependent of the type of fiber. Spatial pitch of the grating is controlled during the manufacturing process and Bragg wavelength can be generated within almost any spectral band of interest. The linear distance between the gratings can be adjusted for the desired sensor placements on the structure. This characteristic is called multiplexing, as is depicted in Figure 3.

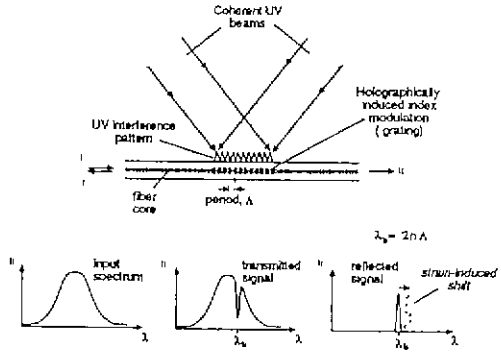

Fig. 2 Transmission and Reflection of FBG

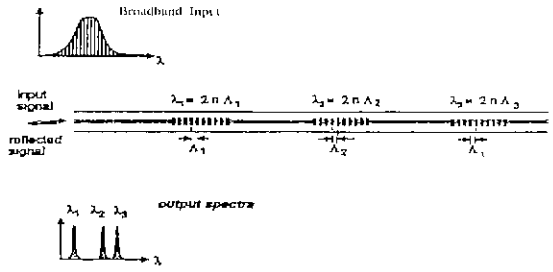

Fig. 3 Multiplexing of FBG sensors

When the deformation is occurring in the structure, shift of spatial pitch changes the wavelength at which the resonance condition is satisfied. The input spectrum from passive broadband optical source is reflected by FBG and the output narrowband spectrum includes the information on the change of resonance wavelength. Strains at each FBG sensors are calculated by filtering an output spectrum and comparing it with that before deformation. This inherent 'wavelength-encoded' nature of the output of FBG has distinct advantages over other sensing schemes.

There are two constraints on the Bragg wavelengths of the sensors in the array. The wavelengths of all gratings multiplexed in an optical fiber should be within the bandwidth of the source. There should not be 'cross-talk': the wavelengths of adjacent gratings must be such that they do not intersect or cross over when the structure is loaded to its maximum load.

3. Testing Procedures and Apparatus

A series of laboratory tests were performed to investigate the possibility of measuring load transfer mechanism of pile by fiber optic sensor. For all the specimens tested, both optical fiber sensor and strain gage were installed at corresponding locations. Preliminary test, such as uniaxial tensile test of steel bar, was carried out. Static pile load tests on three model piles installed in calibration chamber were performed and the distributions of load transfer measured by both measuring system were compared.

3.1 Fabrication of FBG Sensor

There are two typical methods in grating fabrication. One is the holographic writing technique and the other is the phase mask method. The former is not adequate to write gratings of a precise wavelength, since it is difficult to set the interfering angles for a desired wavelength. Therefore, phase mask method, which is simpler for stable grating fabrication, is used in this study. A phase mask grating is fabricated by exposing the UV transmitting silica mask plate to laser beams, followed by dry plasma etching. The grating period is similar to that required for producing the reflection grating in germanium-doped silica. The phase mask diffracts the induced UV beam into 0th, 1st order beams making interference patterns on the fiber core which causes an increase in the local refractive index as in the holographic writing technique. With phase mask method, one can reproduce gratings of the same wavelength that is determined only by the mask period, which is very crucial for mass production. Wavelength of optical fiber is observed with optical spectrum analyzer(OSA) during the process.

Fiber Bragg Gratings used in the study were fabricated at Photonics Research Center at Korea Institute of Science and Technology (KIST). The germanosilicate fiber (KIST-1104, single mode at 1.55 μm, Ge: 18.5 mol.%, B: 22mol.%) was drawn with a modified chemical vapor deposition (MCVD) method. A KrF excimer laser (Lambda Physik, λ=248nm, maximum pulse power=650 mJ) was used as a UV source. The fabrication set-up consisted of a UV laser source, cylindrical lense, mirror and phase mask is shown in Figure 4.

3.2 Uniaxial Tensile Test for instrumented Steel Bar

Both strain gauges and FBG sensors were attached on a cylindrical steel bar, whose diameter and length are 3cm and 50cm respectively. The distance between strain gages was 10cm and FBG sensors were grated at two measuring points. One side of steel bar was machined flat with the width of 1cm and the other one is fabricated with a groove to ensure the bonding between steel and FBG. Optical fiber with FBG is laid straight in a groove and the section of optical fiber except the Bragg gratings is coated by a resin epoxy. And gratings were coated by paraffin to make it respond elastically. The coating with resin epoxy and paraffin also provides the moisture protection for optical fibers.

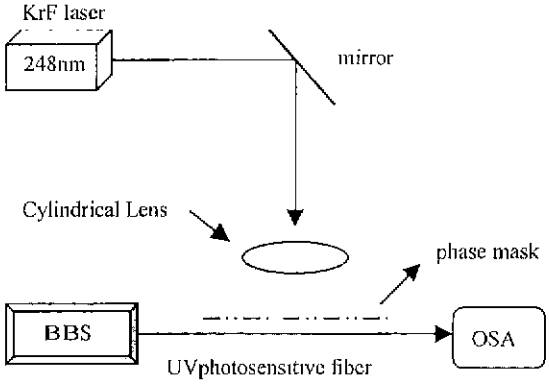

Fig. 4 Set up for Fabrication of FBG

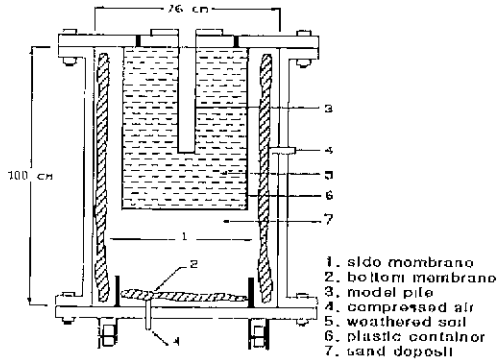

Fig. 5 Pressure Chamber

Tension loading and unloading to the instrumented steel bar were applied by universal testing machine, and the strain measurements by strain gage and FBG were analyzed in terms of linearity and hysteresis. The FBG sensor signal encoding the information on the wavelength was measured using an optical spectrum analyzer(OSA) or a spectrometer. Strain at each FBG sensor was determined by evaluating the variation of resonance wavelength from previous one.

3.3 Model Pile Test

3.3.1 Test Ground

Model ground was prepared by compacting the layers of weathered granite soil, and then model pile was installed in compacted soil through excavation and fabrication of pile material. Weathered granite soil was obtained from Poi-dong, southern part of metropolitan Seoul. Its optimum moisture content and maximum dry density were 16% and 1.9t/m^3, respectively. Weathered granite soil dried in an oven at 105℃ for 24 hours was mixed with water to have optimum moisture content. Then it was compacted in five layers in a plastic box of 60cm high and 40cm diameter, using a metal rammer of 7.5kg weight with a drop height of 60cm. Since the direct compaction of weathered granite soil in the calibration chamber may damage the membranes and compacted granite soil is too stiff to accommodate the stress change at chamber boundaries, a sand deposit is located between the plastic box containing compacted weathered granite soil and the membranes by raining method as shown in Figure 5. Air-dried sand with water content of less than 2% was used and it was poorly graded clean fine sand, classified as SP by the USCS. An upper chamber plate was placed above the surface of sand deposit and tied strongly to prevent a leakage of chamber pressure applied to the model ground in horizontal and vertical directions.

3.3.2 Installation of Model Pile

Excavation for model pile was carried out 24 hours after appling vertical and horizontal pressure through rubber membranes inside the pressure chamber. The procedure to install a model pile in chamber is illustrated in Figure 6. A hole was drilled with an electric screw whose diameter, pitch, and length are 4cm, 6cm and 40cm, respectively. Using this screw drill, compacted weathered granite soil was excavated up to 40cm below the surface with 4cm diameter. Before pouring a mortar, the slime occurred during an excavation was removed by compressed air of 1kg/cm^2

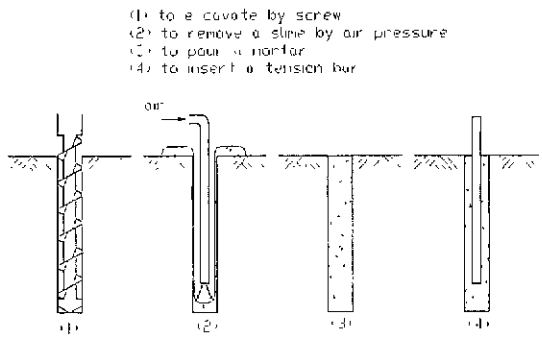

Fig. 6 Installation Procedure of Model Pile

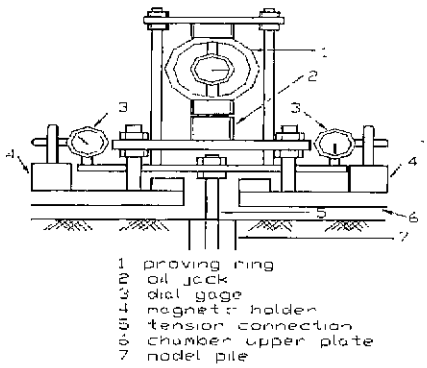

Fig. 7 Loading System for Pile

pressure. A mortar mixture of cement, water, expansive agent and additional materials was poured and compacted by five layers in a drilled hole. Immediately after the injection of mortar, tension bar with a length of 50cm for loading test was inserted into the center of model pile. Model pile was cured for 7 days and the loading test was performed.

3.3.3 Static Load Test on Model Piles

Two tension tests and one compression test were performed, following the procedure of quick maintained load test. The interval of maintained load at each loading stage was 5 minutes and the displacement was checked at 0, 2.5, 4 and 5 minutes. The schematic drawing of tensile loading test system is shown in Figure 7. Load applied by an oil jack of 5 ton maximum capacity was measured by a proving ring which can be loaded up to 3 tons, and displacements at pile butt was measured by two dial gauges

Table 3 Conditions for Model Pile Tests

Pile Type	σ'_h (kg/cm²)	σ'_v (kg/cm²)	K	Pile Length (cm)
P1	0.6	1.0	0.6	36
P2	0 6	0 75	0 8	36 5
P3	0.4	1 0	0.4	37.5

with accuracy of 1/200mm. Three model piles were tested and Table 1 presents the details of test condition.

Piles P1 and P2 were tested in tensile loading system and a compressive load test was performed for P3. For the investigation of load transfer mechanism, electric strain gages and FBG sensors attached on a reinforcing bar were installed in the test piles. To protect the FBG sensors and strain gauges, the reinforcing bar was embedded in a thin-wall metal pipe with a slightly larger diameter than that of reinforcing bar. Metal pipe was removed immediately after the installation of model pile. For tension tests, four strain gages and FBG sensors were attached to a reinforcing bar at 5, 15, 25, 35cm depth. For compression test, they were attached to a reinforcing bar at depths of 5, 20, and 35cm.

4. Test Results and Analysis

4.1 Uniaxial Tensile Test for Steel Bar

The Fiber Bragg Gratings were first calibrated by tension test for steel bar. This calibration was performed for several identical gratings to verify the repeatability of the grating fabrication and gage properties. Figure 8 showing the

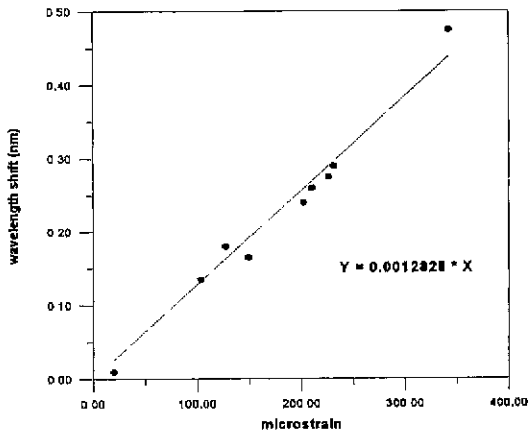

Fig. 8 Wavelength Shift vs. Strain

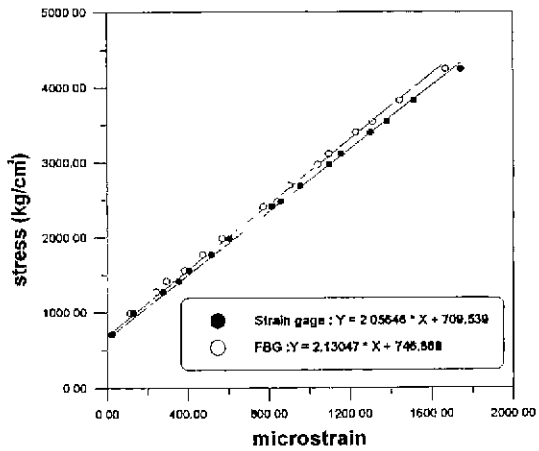

Fig. 9 Stress vs. Strain by FBG and Strain Gage

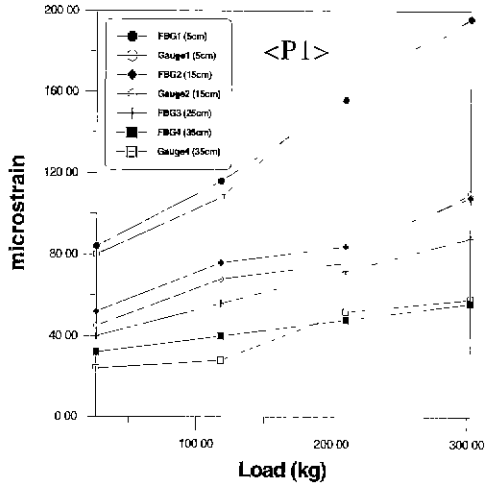

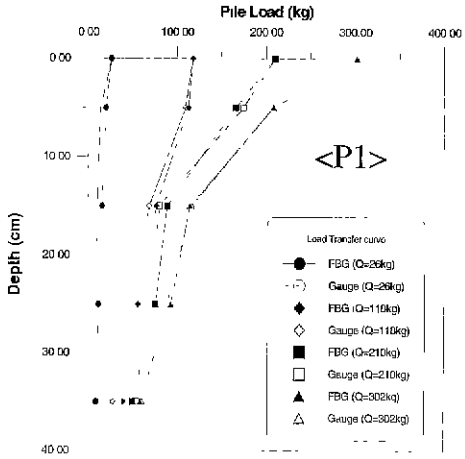

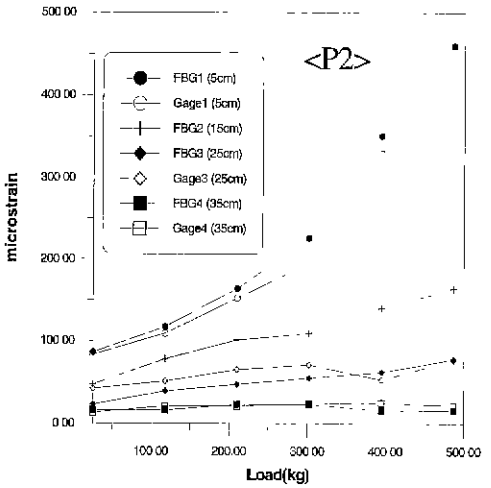

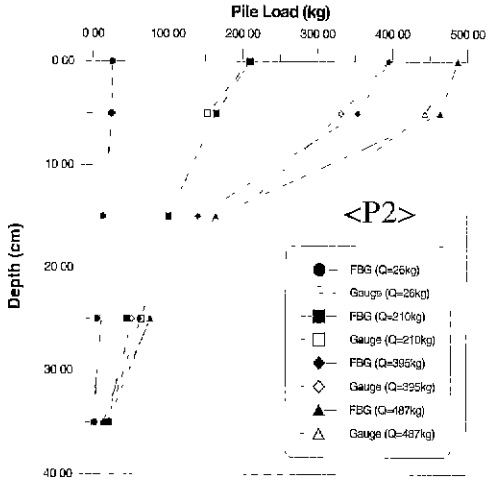

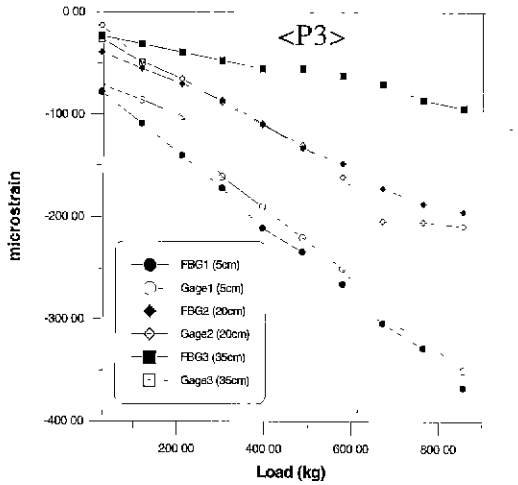

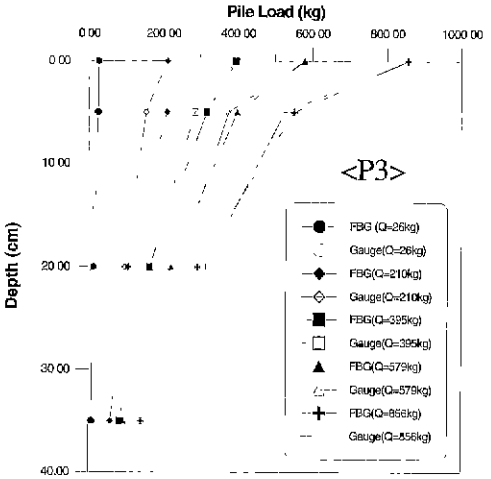

Fig. 10 Comparison of Strain Values

Fig. 11 Comparison of Axial Loads

relation between the shift of wavelength of FBG and the strain measured by strain gage was obtained from the uniaxial tension test for steel bar. The dependence of the return wavelength on strain is obtained by the regression of the measured values, 1.28pm/ μ strain. Here 1 μ strain is an variation of 1 part in 10^6. In other words, wavelength shift is converted into strain by multiplying 780. It can be noted from Figure 9 that the strains measured by FBG sensor are

matched to those of the strain gauge quite well. It is also shown that the trend of stress-strain relationship is similar for both measurements and that there is an insignificant difference in strain values under the loading and unloading steps. An elastic modulus calculated from stress-strain relationship in Figure 9 is approximately 215 GPa and it is similar to 220 GPa given by the manufacturer.

4.2 Load Transfer Mechanism of Model Piles

4.2.1 Comparison of Strain Values

The comparison of strain values measured by two sensor systems were made by plotting them with respect to loads, as shown in Figure 10. It was observed that the difference between two values is within the range of 5%~10%, and both measurements show similar trends. It was also shown that FBG sensor presents smoother trend in measured strains while slightly abrupt changes in measured values by strain gage are detected as loading increases. Minus value of strain in the test results of P3 means that wavelength of FBG sensor decreases in compressive condition.

4.2.2 Distribution of Axial Pile Loads

In order to evaluate the axial pile load distribution along pile penetration depth from measured strains, Young's modulus is determined from the strain gauge located at 5cm below the ground surface as a reference for determining the relation between the measured strain and the load in the pile. Despite of careful installation of tension bar, a strain gage located at a depth of 25cm on P1 pile and a strain gauge at 15cm from top of P2 pile were found not to work after the curing. For P3 pile, strain gage at 35cm depth was broken during load test. From above observations, it appears that the durability of FBG sensor is comparatively good and FBG sensor may have a strong possibility to be a useful tool for monitoring geo-structures in a field.

Axial loads evaluated from load transfer tests on test pile P1, P2 and P3 at each loading stage are obtained in Figure 11. Load for piles P1 and P2 is tension while pile load is compression for P3. From the load transfer mechanism measured, it was shown that the distributions of axial load on three piles were in excellent agreement except at the depths where strain gages were broken. In pile load transfer curves, variation of load represented by a dashed line indicates that strain was not measured due to the strain gage problem. From model pile tests, it was concluded that the use of FBG sensor in monitoring the strain in piles shows great potential for the analysis of pile load transfer with the accuracy.

5. Conclusions

In this research, efforts were made to demonstrate the applicability of fiber optic sensor as an useful sensor system. The general conclusions that can be drawn from test results are summarized as follows.

(1) The dependence of the return wavelength of FBG on strain was 1.28pm/μstrain and it showed a relatively good agreement in correlation between two sensor systems.

(2) In model pile tests, the difference between two values was less than 5%~10%. FBG sensor presented the smoother trend in measuring values while slightly abrupt trend was detected in strain gage as pile load tests were proceeded. When it comes to distribution of pile axial load, three piles showed a good agreement except at several depths where strain gages malfunctioned.

(3) It was shown that FBG sensor has a sufficient potential for the application to measure pile load transfer. However, since FBG sensor is sensitive to temperature, it needs to take side-effect due to temperature consideration into evaluating pile load precisely. Also, more advanced embedding method should be developed for the use of FBG sensor in field work.

References

1. Aboutaha, M., Roeck, G. D., and Van Impe, W F. (1993), "Bored versus Displacement Piles in Sand-experimental Study", Deep Foundation on Bored and Auger Piles, pp.157~162.
2. Claus, R. O., and Murphy K. A. (1993), "Optical Fiber Sensors for the Quantitative Measurement of Strain in Reinforced Concrete Structures", Experiments in Smart Materials and Structures, ASME, Vol. 181, pp.97~101.

3. Dandridge, A., Cole, J. H., and Siegel Jr., G. H. (1984), Optical Fiber Sensors. Technical Digest-Symposium on Optical Fiber Measurements, pp.49～54.
4. Kleyner, I. M., and Krizek, R. J. (1995), "Mathematical Model for Bore-Injected Cement Grout Installations", Journal of Geotechnical Engineering, Vol. 121, No. 11, pp.782～788.
5. Kulhawy, F. H. and Turner J. P. (1989), "Load Transfer in Deep Foundations under Repeated Axial Loading", Foundation Engineering, Vol I, pp.511～525.
6. Morse, T. F. and Reinhart L. J. (1993), "Experimental Results on Embedded Optical Fiber Sensors in Concrete", Experiments in Smart Materials and Structures, ASME, Vol. 181, pp.53～60.
7. Oh, J. H. (1999), "Measurement of Pile Load Transfer using Fiber Bragg Grating Optical Sensors", M. Sc Thesis, Korea Univ, Seoul, Korea.
8. O'Neill, M. W. and Raines, R. D.(1991), "Load Transfer for Pipe Piles in Highly Pressured Dense Sand", Journal of Geotechnical Engineering Division, ASCE, Vol. 117, No. 8, pp.1208～1226.
9. Ostrander, K. A. (1990), "Application of Fiber Optics in Strain Measurements of Structures", M. Sc. Thesis, University of Colorado, Boulder, U.S.A.
10. Sirkis, J. S. (1999), "Optical Fiber Strain Sensing in Engineering Mechanics", Short Course Notes, SPIE's International Symposium on Smart Structures, Newport Beach, CA.
11. Yoon, S S. (1998), "An Experimental Study on the Characteristics of Bearing Capacity of Auger-cast Pile Installed using Expansive Mortar", M. Sc. Thesis, Korea Univ., Seoul, Korea.

(접수일자 2000. 5. 25)